PHYSICAL REVIEW B VOLUME 17, NUMBER 4 15 FEBRUARY 1978

Electronic states at unrelaxed and relaxed GaAs (110) surfaces

Eugene J. Mele and J. D. Joannopoulos
Department of Physics, Research Laboratory of Electronics, Massachusetts Institute of Technology, Cambridge, Massachusetts 02139
(Received 4 May 1977)

We have shown that, using a general class of Hamiltonians, the transfer-matrix technique may be used to obtain exact solutions for the electronic states at any crystal surface bounded by semi-infinite bulk. This result is formally generalized as a theorem and is used to study the electronic states at a clean GaAs (110) surface. The calculation employs an empirical tight-binding Hamiltonian which realistically models the GaAs surface and allows meaningful comparison with both experiments and self-consistent pseudopotential calculations. Surface states are calculated for the clean (110) surface, and a variety of structural relaxations are studied.

I. INTRODUCTION

The investigation of the nature of electronic states at semiconductor surfaces is a matter of both theoretical interest and practical importance. Theoretically, the existence of a surface hinders the application of conventional band-structure methods to the calculation of electronic properties of such systems. Recently, such systems have been modelled by periodically repeating in real-space finite "slabs" bounded by vacuum layers on both sides.[1,2,10-13] This strategy provides artificial periodicity at the expense of introducing a large unit cell; surface calculations using both the empirical tight-binding method as well as self-consistent pseudopotentials have been performed in this way Surface pseudopotential calculations have also been performed by matching surface wave functions to bulk wave functions, parametrized in a complex wave vector, at some depth into the bulk.[3] Recently, the first calculations using a tight-binding model on a truly semi-infinite crystal have been performed by applying the transfer-function technique to very simple tight-binding Hamiltonians.[4-6] We report here the first extension of such a method to a realistic tight-binding model for a semiconductor surface. We note first of all that the transfer-matrix technique is quite general; using a Hamiltonian of finite range, exact solutions for the electronic states of any crystal surface may be obtained using this method. This result can be stated as a theorem, and we have applied it to the study of surface states at the (110) face of GaAs. Calculations have been performed for both the unrelaxed surface and for the surface under a variety of relaxations. We define relaxations as any movement of surface atoms that leave the surface unit cell invariant.

The plan of this paper is as follows. First, we discuss the formalism and introduce a theorem for the calculation of electronic states at the surface of a semi-infinite crystal. Secondly, we will briefly discuss the empirical tight-binding Hamiltonian for the GaAs (110) surface. Thirdly, we will discuss calculations for the unrelaxed (110) surface, presenting level by level local densities of states to study the decay of surface bands into the bulk. Fourth, we investigate the effects of several relaxations on the surface states with this Hamiltonian. In this study of relaxations at the (110) surface, we find that the dangling-bond surface states are pushed to the band-gap edges only for a relaxation in which the surface cation attains a planar configuration with its nearest neighbors. Finally, we conclude with a summary of these surface calculations and their extension to theoretical adsorption studies on GaAs (110) surfaces.

II. FORMALISM

The termination of a crystal at a surface is a unique type of periodicity breaking perturbation; namely, in the absence of surface reconstruction we retain the full periodicity of the crystal parallel to the surface plane. In the direction normal to the surface we have a regular, though nonperiodic, configuration. This regularity parallel to the surface normal allows an *exact* solution for the surface electronic spectrum for a general *class* of Hamiltonians. This possibility has been previously recognized and pursued only for simple tight-binding Hamiltonians with which the "equations of motion" are solved relatively straightforwardly. Here we present this formalism quite generally, with a general prescription for the solution of the surface equations and with subsequent application to a realistic model for a (110) zincblende surface.

Consider a set of n_t complete localized Bloch orbitals (in a two-dimensional k vector), $\{\psi_{n_t}^{l_L}(\vec{k}, \vec{r} - \vec{\tau}_t)\}$, for each atom at position $\vec{\tau}_t$ in the surface primitive cell for an infinite set of layers

L parallel to the surface with sublayer index $\{l_L = 1, 2, \ldots, N\}$. The Bloch orbitals interact through the Hamiltonian

$$H^{l_L, l'_{L'}}_{n_l, n'_{l'}}(\vec{k}) = \langle \psi^{l_L}_{n_l}(\vec{k}, \vec{r} - \vec{\tau}_l) | H | \psi^{l'_{L'}}_{n'_{l'}}(\vec{k}, \vec{r} - \vec{\tau}_{l'}) \rangle \quad . \tag{1}$$

We wish to choose N to be the minimum number such that

$$H^{l_L, l'_{L'\pm 2}}_{n_l, n_{l'}}(\vec{k}) = 0; \quad H^{l_L, l'_{L'\pm 1}}_{n_l, n_{l'}} = H^{l_{L'}, l'_{L'\pm 1}}_{n_l, n_{l'}} \tag{2}$$

for all L and L' not equal to zero. That is, principal layers L and $L \pm 2$ are totally uncoupled. For $L = 0$ one chooses a cell large enough to satisfy the first condition, although the second condition is not in general satisfied at $L = 0$. This truncation formally reduces the general surface problem to a one dimensional semi-infinite chain, a problem which is exactly solvable.

If Eq. (2) is applicable, this reduction is *always* possible for a surface problem. The solution proceeds as follows: we define the Green's function matrix elements

$$G^{l_L, l'_{L'}}_{n_l, n_{l'}} = (\epsilon - H)^{-1} \Big|^{l_L, l'_{L'}}_{n_l, n_{l'}} \quad , \tag{3}$$

where n_l denotes the nth orbital in layer l. We can apply Dyson's equation at the Lth layer to obtain

$$\epsilon G^{l_L, l'_0}_{n_l, n'_{l'}} = \delta_{L0} \delta_{l_L l'_0} \delta_{n_l, n_{l'}} + \sum_{n=-1}^{1} \sum_{l''_{L+n}, n_{l''}} H^{l_L, l''_{L+n}}_{n_l, n_{l''}} G^{l''_{L+n}, l'_0}_{n_{l''}, n_{l'}} \quad . \tag{4}$$

Here we define the transfer function T such that

$$G^{l_{L+1}, l'_0}_{n_l, n_{l'}} = \sum_{l''_L, n_{l''}} T^{l_{L+1}, l''_L}_{n_l, n_{l''}} G^{l''_L, l'_0}_{n_{l''}, n_{l'}} \quad . \tag{5}$$

Then, by combining Eqs. (4) and (5) we obtain a self-consistency requirement on T,

$$T = (\epsilon - H_{LL} - H_{L, L+1} T)^{-1} H_{L, L-1} \quad . \tag{6}$$

Here the product implies summation over all intermediate l_L and n_l. H_{LL} restricts the Hamiltonian of Eq. (1) to $L = L'$; similarly, $H_{L, L+1}$ denotes an *inter*principal layer interaction. For very simple systems Eq. (6) can be solved directly to obtain T. For more complicated systems, one can always obtain an exact numerical solution by iteration with the initial guess that T is zero. In either case T is specified by Eq. (6).

Once T is obtained the surface Green's function is straightforwardly calculated from Dyson's equation. Because of the generality of the approach we state this result as a theorem. *Theorem*: for the class of Hamiltonians which satisfy the restrictions of Eq. (2), the Green's function at the surface layer (indexed $L = 0$) has the form

$$G^{l_0, l'_0}_{n_l, n_{l'}}(\vec{k}, \epsilon) = \{ [\epsilon - H_{00}(\vec{k}) - H_{01}(\vec{k}) \cdot T(\vec{k}, \epsilon)]^{-1} \}^{l_0, l'_0}_{n_l, n_{l'}} , \tag{7}$$

where T is the transfer function specified by Eq. (6).

Two similar and quite useful results also follow directly. Firstly, for a surface relaxation, where $H_{00} \neq H_{11} = H_{22} \cdots$ and $H_{01} \neq H_{12} = H_{23} \cdots$, the Green's function at the surface layer is given by

$$G^{l_0, l'_0}_{n_l, n_{l'}}(\vec{k}, \epsilon) = (\{ \epsilon - H_{00}(\vec{k}) - H_{01}(\vec{k}) \cdot [\epsilon - H_{12}(\vec{k}) T(\vec{k}, \epsilon)]^{-1} \cdot H^{\dagger}_{01}(\vec{k}) \}^{-1})^{l_0, l'_0}_{n_l, n_{l'}} \quad . \tag{8}$$

Secondly, the bulk Green's function at layer L is given by

$$G^{l_L, l'_L}_{n_l, n_{l'}}(\vec{k}, \epsilon) = \{ [\epsilon - H_{L, L+1}(\vec{k}) T(\vec{k}, \epsilon) - H_{L, L-1}(\vec{k}) \cdot T'(\vec{k}, \epsilon)]^{-1} \}^{l'_L, l_L}_{n_l, n_{l'}} \quad . \tag{9}$$

To define T' note that in general there exists a unitary transformation which relates $[\psi^{l_L}_{n_l}(\vec{k}, \vec{r} - \vec{\tau}_l)]$ to the basis functions in the Lth cell after a mirror inversion of the Lth cell about the surface axis. Calling this transformation S, then

$$T'(\vec{k}, \epsilon) = S^{\dagger} T(\vec{k}, \epsilon) S \quad . \tag{10}$$

Finally, once the Green's functions are obtained, physical quantities such as densities of states and charge densities are calculable in the usual way.

III. TIGHT-BINDING MODEL

We have applied this formalism to the (110) surface of GaAs employing a nine-parameter empirical tight-binding Hamiltonian. Some features of this approach are worthy of note.

Firstly, it is generally acknowledged that such empirical tight-binding calculations are at least pedagogically useful. We emphasize, in addition, that such calculations can be very realistic; such models can be chosen to represent the valence bands very well. The model we have used parametrizes all distinct nearest-neighbor interactions.[7] These interactions are shown schematically in Fig. 1, and the values used are tabulated in Table I. Note that the lack of inversion symmetry requires additional parameters describing both the separation in orbital self-energies and the two types of sp_σ interactions be-

TABLE I. Nearest-neighbor empirical tight-binding parameters for GaAs. The interaction parameters are given schematically in Fig. 1.

E_0^a	E_0^c	V_1^a	V_1^c	V_2	V_3	V_4	V_5	V_6
−0.98	2.59	−2.42	−1.61	−5.07	−0.26	0.03	0.58	−0.46

tween nearest-neighbor sites. Hence we require four more parameters than for the corresponding homopolar system. This model yields the energy eigenvalues at high-symmetry points tabulated in Table II. In this table we compare these results to eigenvalues obtained from the pseudopotential calculations of Chelikowsky and Cohen.[8] Note that the agreement is generally good and can be improved by including second-nearest-neighbor interactions. Furthermore, while the failure of such models to adequately represent the conduction bands is generally cited as a shortcoming, we note that inclusion of a single basis function representing an excited, bound, anionlike s state provides a good description of even the lowest conduction band, with little effect on the valence levels.[9] We conclude that such models provide a reasonable approach to the study of electronic phenomena near or below the conduction-band edge.

Secondly, such tight-binding models are well suited to the study of more complex phenomena involving semiconducting surfaces, such as surface relaxation, reconstruction, and adsorption.[10] The formulation of such problems through the construction of localized real-space interactions facilitates an understanding of the essential variations in electronic surface states under such perturbations. This is especially true for the study of surface chemisorption where one expects local, chemical, molecularlike effects to most strongly influence the results. Further, the tractability of the method makes possible the study of a wide range of surface geometries and adsorbate configurations.

Thirdly, tight-binding studies of the GaAs surface using truly realistic Hamiltonians are only currently becoming available. Two early tight-binding calculations have been reported for this surface.[11,12] However, the first of these was actually a general treatment of the (110) surface of all heteropolar zincblendes, and hence the parameters chosen do not quantitatively describe the specific nature (i.e., fundamental gap width, heteropolar gap width, valence band width, etc.) of the GaAs crystal. The second of these calculations proceeded with a Hamiltonian which anomalously ordered the anion and cation p-orbital energies. This ordering is noteworthy, because a crystal calculation with this Hamiltonian would predict a valence band with largely cation p character, a significant result in conflict with both experimental and self-consistent pseudopotential results. The parameters used in the present calculation are chosen to fit the pseudopotential bulk band structure, while maintaining the free atomic ordering of the basis orbital self-energies.[7] By this we mean (as may be calculated from the data in Table I) that the orbital self-

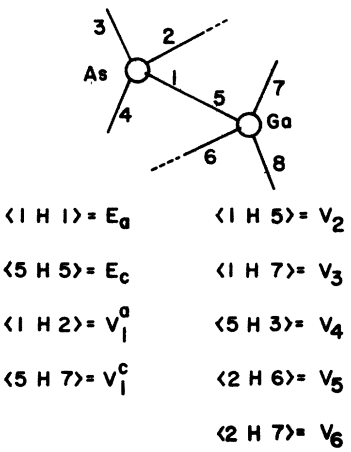

FIG. 1. Schematic definition of the basis orbitals and interaction parameters in this model.

TABLE II. Comparison of eigenvalues at bulk symmetry points obtained from the model of Table I with nonlocal pseudopotential eigenvalues.

	Pseudopotential	Tight-binding model
Γ_1^V	−12.55	−12.89
$\Gamma_{2,3,4}^V$	−0.35(1) 0.00(2)	−0.02(3)
Γ_1^C	1.51	1.65
$\Gamma_{2,3,4}^C$	4.55(2) 4.71(1)	4.57(3)
X_1^V	−9.83	−9.71
X_2^V	−6.88	−6.79
$X_{3,4}^V$	−2.99 −2.89	−4.01
X_1^C	2.03	4.84
L_1^V	−10.60	−10.82
L_2^V	−6.83	−6.64
$L_{3,4}^V$	−1.42 −1.20	−1.96
L_1^C	1.82	2.17

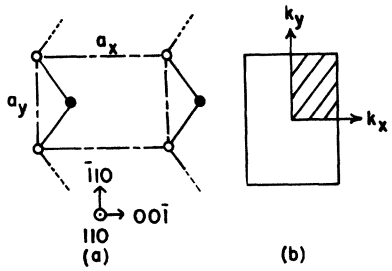

FIG. 2. (a) (110) surface unit cell for GaAs, $a_x = 5.68$ Å, $a_y = 4.00$ Å; (b) the (110) surface Brillouin zone; the shaded region is the irreducible zone.

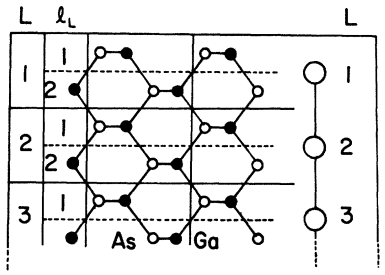

FIG. 3. (110) surface as viewed from the [1$\bar{1}$0] direction. Dashed lines depict reduction to one-dimensional chainlike system on the right. The left-hand panel defines the principal layer index L and the sublayer index l.

energies are ordered in increasing value: anion 4s, cation 4s, anion 4p, and cation 4p. Furthermore, the s-p energy splitting for the anion exceeds the same splitting as the cation as expected from the free-atom term values. Note that one may attribute the slight deviations of the orbital self-energies from the exact isolated atom energies to a variety of solid-state effects including charge transfer and the assumption of site to site orthogonality in the tight-binding model. Concurrent with this study, and independent of it, are several tight-binding calculations for this surface using realistic Hamiltonians,[7,10,12] which are currently being published. The calculation of Ref. 12(b) is noteworthy in that an attempt is made to model the effects of charge transfer and Madelung potential at the surface. While these corrections are more significant for the more ionic II–VI compound ZnSe, which is also calculated in this way, we find that the correction for GaAs which is quite covalent in character is quite small. In general, we find that our model is sufficiently realistic to allow meaningful comparison with both experiments and self-consistent pseudopotential calculations.

In conclusion, we emphasize that empirical tight-binding studies of surface electronic properties are useful because they may be quite realistic, they are a natural vehicle for the investigation of a variety of surface perturbations including relaxation, adsorption, etc., and finally they are tractable. This work provides an approach complementary to the more exact pseudopotential formalism.

IV. APPLICATION TO GaAs (110)

In Fig. 3 we show the (110) surface as viewed from the [1$\bar{1}$0] direction. The horizontal solid lines represent the boundaries of principal layers L which can be further subdivided into two sublayers l_L each. The vertical solid lines represent the primitive cell boundaries. Although these are not the simplest choices of principal layers and primitive cell, they are instructive in illustrating the applications of the methods discussed in Sec. II for more complicated systems.

Using Eq. (7) of the theorem, the Green's function at the surface principal layer can be immediately rewritten as

$$\begin{pmatrix} G^{l_0,l_0} & G^{l_0,l_0'} \\ G^{l_0',l_0} & G^{l_0',l_0'} \end{pmatrix} = \left[\begin{pmatrix} \epsilon - E_0 & \alpha^\dagger \\ \alpha & \epsilon - E_0 \end{pmatrix} - \begin{pmatrix} 0 & 0 \\ \beta & 0 \end{pmatrix} \begin{pmatrix} T^{l,l} & T^{l,l'} \\ T^{l',l} & T^{l',l'} \end{pmatrix} \right]^{-1}, \tag{11}$$

where all the elements are actually 8×8 matrices obtained using the Hamiltonian discussed in Sec. III. To define these elements, we label the basic orbitals in each sublayer one through eight where in terms of anion and cation s and p orbitals

$$\begin{aligned} h_1 &= \tfrac{1}{2}(s^a + p_x^a - p_y^a - p_z^a) , \\ h_2 &= \tfrac{1}{2}(s^a - p_x^a + p_y^a - p_z^a) , \\ h_3 &= \tfrac{1}{2}(s^a + p_x^a + p_y^a + p_z^a) , \\ h_4 &= \tfrac{1}{2}(s^a - p_x^a - p_y^a + p_z^a) , \\ h_5 &= \tfrac{1}{2}(s^c - p_x^c + p_y^c + p_z^c) , \\ h_6 &= \tfrac{1}{2}(s^c + p_x^c - p_y^c + p_z^c) , \\ h_7 &= \tfrac{1}{2}(s^c + p_x^c + p_y^c - p_z^c) , \\ h_8 &= \tfrac{1}{2}(s^c - p_x^c - p_y^c - p_z^c) . \end{aligned} \tag{12}$$

With this ordering we can write E_0, α, β in blocks of 4×4 matrices.

$$E_0 = \begin{pmatrix} E_A & H_L \\ H_L^\dagger & E_C \end{pmatrix} , \tag{13}$$

$$\alpha^\dagger = \begin{pmatrix} 0 & H_E \eta^* \xi^* \\ H_D & 0 \end{pmatrix} , \tag{14}$$

$$\beta=\begin{pmatrix} 0 & H_E \\ H_D\eta\,\xi & 0 \end{pmatrix}, \tag{15}$$

where

$$E_A=\begin{bmatrix} E_0^a & V_1^a & V_1^a & V_1^a \\ V_1^a & E_0^a & V_1^a & V_1^a \\ V_1^a & V_1^a & E_0^a & V_1^a \\ V_1^a & V_1^a & V_1^a & E_0^a \end{bmatrix}, \tag{16}$$

$$E_C=\begin{bmatrix} E_0^c & V_1^c & V_1^c & V_1^c \\ V_1^c & E_0^c & V_1^c & V_1^c \\ V_1^c & V_1^c & E_0^c & V_1^c \\ V_1^c & V_1^c & V_1^c & E_0^c \end{bmatrix}, \tag{17}$$

$$H_L=\begin{bmatrix} V_2+V_5\eta^* & V_3+V_4\eta^* & V_3+V_6\eta^* & V_3+V_6\eta^* \\ V_4+V_3\eta^* & V_5+V_2\eta^* & V_6+V_3\eta^* & V_6+V_3\eta^* \\ V_4+V_6\eta^* & V_6+V_4\eta^* & V_6+V_6\eta^* & V_5+V_5\eta^* \\ V_4+V_6\eta^* & V_6+V_4\eta^* & V_5+V_5\eta^* & V_6+V_6\eta^* \end{bmatrix}, \tag{18}$$

$$H_E=\begin{bmatrix} V_5 & V_6 & V_4 & V_6 \\ V_6 & V_5 & V_4 & V_6 \\ V_6 & V_6 & V_4 & V_5 \\ V_3 & V_3 & V_2 & V_3 \end{bmatrix}, \tag{19}$$

$$H_D=\begin{bmatrix} V_5 & V_6 & V_3 & V_6 \\ V_6 & V_5 & V_3 & V_6 \\ V_6 & V_6 & V_3 & V_5 \\ V_4 & V_4 & V_2 & V_4 \end{bmatrix}. \tag{20}$$

Here, $\eta=e^{ik_y a_y}$ and $\xi=e^{ik_x a_x}$ are the phases associated with translation across one unit cell in the $[1\bar{1}0]$ and $[00\bar{1}]$ directions, respectively (Fig. 2).

To solve for the transfer matrix, we rewrite Eq. (6) in the form

$$\begin{pmatrix} T^{ll} & T^{ll'} \\ T^{l'l} & T^{l'l'} \end{pmatrix}=\left[\begin{pmatrix} \epsilon-E_0 & \alpha^\dagger \\ -\alpha & \epsilon-E_0 \end{pmatrix}-\begin{pmatrix} 0 & 0 \\ \beta & 0 \end{pmatrix}\times\begin{pmatrix} T^{ll} & T^{ll'} \\ T^{l'l} & T^{l'l'} \end{pmatrix}\right]^{-1}\begin{pmatrix} 0 & \beta^\dagger \\ 0 & 0 \end{pmatrix}. \tag{21}$$

By inspection and from the symmetry of the Hamiltonian, the solution to Eq. (21) reduces to the simple form

$$\begin{pmatrix} T^{ll} & T^{ll'} \\ T^{l'l} & T^{l'l'} \end{pmatrix}=\begin{pmatrix} 0 & T_1 \\ 0 & T_2T_1 \end{pmatrix}, \tag{22}$$

and therefore with a little algebra, one obtains

$$T_2=[\,\epsilon-E_0-\beta(\epsilon-E_0-\alpha^\dagger T_2)^{-1}\beta^\dagger\,]^{-1}\,\alpha \tag{23}$$

and

$$T_1=(\epsilon-E_0-\alpha^\dagger T_2)^{-1}\beta^\dagger\ . \tag{24}$$

These equations are simultaneously solved by iteration as noted in Sec. II.

Once the converged solution for $T_2(\vec{k},E)$ is obtained, the surface (principal layer $L=0$, sublayer $l_0=0$) density of states is obtained from

$$n_s(E)=-\frac{2}{\pi}\int d^2k\,\mathrm{Im}\,\mathrm{Tr}\,G^{0,0}(k,E)\big|_{L=0}\,, \tag{25}$$

or

$$n_s(E)=-\frac{2}{\pi}\int d^2k\,\mathrm{Im}\,\mathrm{Tr}(E-E_0-\alpha^\dagger T_2)^{-1}\ . \tag{26}$$

Finally, it is also useful to use this formalism to compute the local density of states at an arbitrary layer into the bulk. This can be accomplished by a straightforward solution to the linear Eqs. (4) with l_0 replaced by a desired sublayer index l_M. Such a solution requires $\sim M$ inversions of matrices of the dimension of G (16 in this case) at each energy. This tedious solution can be avoided by the following approach.

First, to avoid a cumbersome notation, label sublayers l_M by a single index $N=2M+l$. Hence, each sublayer is identified by a single superscript. Then, given $G^{N-1,N-1}(\vec{k},E)$, we wish to compute $G^{N,N}(\vec{k},E)$. Assume N is odd. For this case

$$(E-E_0)G^{N,N}(\vec{k},E)=1+\beta G^{N+1,N}(\vec{k},E)+\alpha G^{N-1,N}(\vec{k},E)\,, \tag{27}$$

or

$$(E-E_0-\beta T_1)G^{N,N}(\vec{k},E)=1+\alpha G^{N-1,N}(\vec{k},E)\ . \tag{28}$$

However, the Hermiticity of the Hamiltonian provides that

$$G^{N-1,N}(\vec{k},E)=[\,G^{N,N-1}(-\vec{k},E)\,]^T\,, \tag{29}$$

or, from the definition of $T_2(\vec{k},E)$

$$G^{N-1,N}(\vec{k},E)=[\,T_2(-\vec{k},E)G^{N-1,N-1}(-\vec{k},E)\,]^T=G^{N-1,N-1}(\vec{k},E)T_2^T(-\vec{k},E)\ . \tag{30}$$

Hence, we must essentially compute $T_2(-\vec{k},E)$. To do this, note that

$$G^{0,0}(\vec{k},E)=G^{0,0}(-\vec{k},E)^T\,, \tag{31}$$

or

$$E-E_0(\vec{k})-\alpha^\dagger(\vec{k})T_2(\vec{k},E)=[\,E-E_0(-\vec{k})-\alpha^\dagger(-\vec{k})T_2(-\vec{k},E)\,]^T\ . \tag{32}$$

Hence,

$$T_2^T(-\vec{k},E)=\alpha^\dagger(\vec{k})T_2(\vec{k},E)\alpha^{-1}(\vec{k})\ . \tag{33}$$

We can straightforwardly use Eq. (29) to obtain

$$G^{N,N}(\vec{k},E)=(E-E_0-\beta T_1)^{-1}\times[1+\alpha^\dagger G^{N-1,N-1}(\vec{k},E)\alpha^\dagger T_2\alpha^{-1}]\ . \tag{34}$$

A similar derivation for N even yields

$$G^{N,N}(\vec{k},E)=(E-E_0-\alpha^\dagger T_2)^{-1}\times[1+\beta^\dagger G^{N-1,N-1}(\vec{k},E)\beta T_1(\beta^T)^{-1}]\ . \tag{35}$$

Using Eqs. (34) and (35) the local density of states at any layer into the bulk can be computed iteratively without completely solving the set of linear Eqs. (4). Hence, this approach is considerably more efficient, especially for a moderately complicated system.

V. RESULTS FOR THE UNRELAXED GaAs (110) SURFACE

In this section, we present the results of the calculation outlined in Sec. IV. Using the Hamiltonian described in Sec. III solutions to Eq. (11) are obtained in the energy range from −14 to 4 eV in 0.1-eV increments over a grid of 25 points in the irreducible Brillouin zone. These data are stored on magnetic tape and retrieved for all of the following surface calculations.

In Fig. 4, we present local densities of states for the surface layer and for six subsequent layers into the bulk, as well as the bulk density of states of GaAs. On each layer we have partially traced the Green's function over the anion and cation to separate out the arsenic and gallium contributions to the local density of states, respectively. The shaded regions represent regions of the spectrum where the surface density of states is large due to the presence of intrinsic surface states.

First, we observe two sharp surface bands in the fundamental gap. The lower of these bands is filled and is strongly As-like in character. The character of this state is mainly p-like on the surface anion and is directed along the "dangling-bond" direction for the anion. The upper state is unfilled and is cation derived. Here the state has a larger fractional s character than the lower state, but still has a large contribution from the Ga p orbitals pointing along the dangling bond. In fact, the ratio of the strengths of the projections of this state on the Ga s and Ga p orbitals is about unity. Note that in this sense neither gap state is strictly dangling hybrid like. The anion state is more p-like; the cation state more s-like.

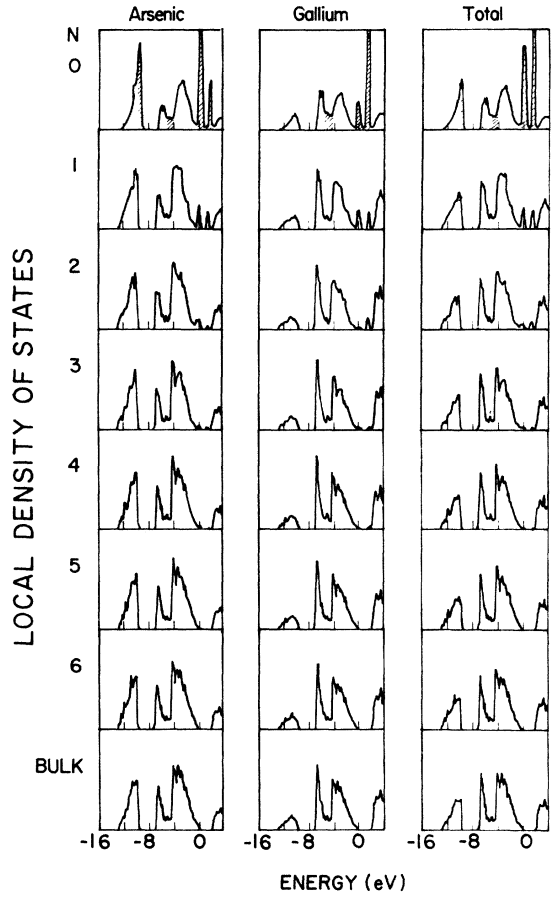

FIG. 4. Local densities of states (LDOS) for the (110) surface sublayer; six subsequent sublayers and bulk for GaAs. On each layer, the LDOS is projected separately onto the anion and cation.

Secondly, at the bottom of the heteropolar gap near −10 eV we find a very strong surface state localized on the As s orbital. Within the resolution of this calculation it is impossible to say whether this state is within the heteropolar gap or below the s band edge in this region of the spectrum.

Thirdly, in the region near −6 eV, we observe a weak, broad surface resonance. These states project strongly on to the surface Ga s orbitals and surface As p orbitals in the (110) plane. Further, this band is wider than the other surface features, as it is resonant with delocalized bulk states at the same energy.

A dramatic feature of Fig. 4 is the rapid decay of these surface features into the bulk. By the fourth layer, the effects of the surface are barely discernible. This establishes the credibility of finite slab calculations for slab thicknesses greater than seven layers, since we find that these sur-

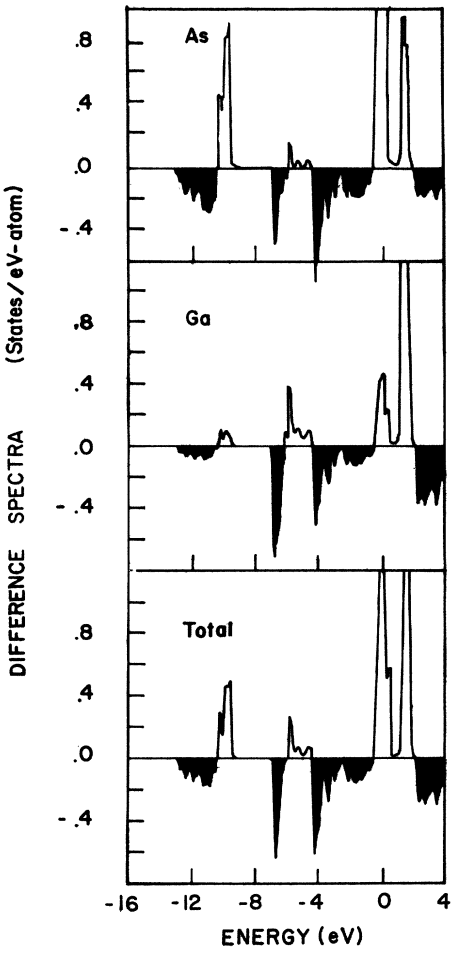

FIG. 5. Difference spectra obtained by subtracting bulk density of states from the surface density of states. Difference spectra clearly show four intrinsic surface-derived bands, and bulk states which are "depleted" at the surface.

face bands require ~3–4 atomic layers to dissipate.

To demonstrate surface-derived features of the density of states more clearly, we have computed a difference spectrum, i.e., calculated

$$n(E) = n_s(E) - n_{\text{bulk}}(E) . \tag{36}$$

Again, these spectra have been partially traced over the anion and cation to distinguish their contributions. The difference spectra are shown in Fig. 5. Note the presence of the four distinct bands previously discussed.

The bands are roughly of equal width (i.e., about 1 eV) except for the weak resonance near −6 eV, which is about 2 eV wide. In addition, the shaded regions depict regions where the difference spectrum is less than zero and hence depict the bulk energies from which the surface states arise. Thus, it is clear that the surface band near −10 eV derives from the lower anion s band. Similarly the broad resonance near −6 eV arises from bulk states slightly lower in energy. This bulk region is gallium s-like in character with strong anion p mixing, consistent with the character previously quoted for this surface state. The lower band-gap state derives from the anion p-like region of the bulk spectrum, but principally from states near −4 eV rather than band-edge states. This is easily understood by noting that the upper valence-band p-like states are π-like in character (i.e., doubly degenerate from Γ to L), while the anion p states *lower* in energy *are more* strongly perturbed by σ-like interactions between p states and sp mixing between sites. Finally, the upper band-gap surface state appears to derive from states near the conduction-band edge. In general, we note that the surface states are displaced towards the fundamental gap relative to their bulk counterparts as one would expect.

Finally, to quantitatively study the decay of these surface features into the bulk, we have computed difference spectra of the form Eq. (36) for each layer into the bulk and integrated the spectra over each positive region separately. As we expect the surface-derived features to decay exponentially into the bulk, we have plotted the natural logarithm of the surface-state "strength" versus depth into the crystal. This plot is shown in Fig. 6 and yields the decay constants tabulated in Table III. The strengths of the surface features near −6 eV were too weak to yield meaningful results by this analysis. We find that the surface states of higher energy decay systematically faster into the bulk. This is reasonable since we note that the energy distribution of the states at lower energy (i.e., the anion s states) is similar

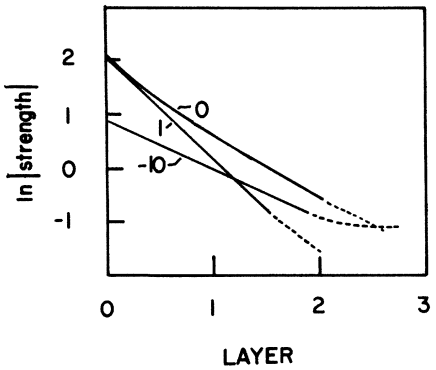

FIG. 6. Plot of the natural log of surface state "strength" vs depth in the bulk. This analysis yields the wave-function decay constants in Table III.

TABLE III. Average decay constants for surface bands obtained from Fig. 6.

Energy	Decay constant
−10.0 eV	−0.23 Å^{-1}
0.0 eV	−0.38 Å^{-1}
1.0 eV	−0.45 Å^{-1}

to the energy distribution of these states calculated in the bulk. This indicates that these surface states are less perturbed by the surface and hence less localized near the edge of the crystal. All of the decay constants are on the order of 0.4 Å^{-1}, hence after 6–7 Å (or 4–5 layers) into the bulk all surface-derived features of the density of states have healed.

The results of this calculation are in very good agreement with the self-consistent pseudopotential work of Ref. 13. As in the pseudopotential calculation, we find a significant increase in the s character of the upper unfilled cation-derived band-gap surface state as compared to the lower anion-like state in the gap.

However, experimentally there is some controversy over the existence of an empty band of surface states in the gap for the clean GaAs (110) surface. Contact potential measurements between n-GaAs and p-GaAs have consistently demonstrated a small, if nonzero, density of surface states in the gap.[14] Photoemission studies have yielded conflicting evidence concerning this problem with some very recent work yielding no observation of band-gap states.[15,16] Further, there has recently been some speculation that photoemission studies which suggest Fermi-level pinning near midgap may be affected by the quality of the cleave obtained, though this work obtains a nonzero density of cation-derived states in the upper gap.[17] Assuming that the density of empty surface states in the gap is small, we wish to investigate the effects of structural rearrangement on the positions of the bandgap states. This problem is addressed in Sec. VI.

VI. RELAXATION

Although both pseudopotential and tight-binding calculations for the ideal GaAs (110) surface yield both filled and unfilled surface bands in the gap, experimental studies which have failed to observe such strong features suggest that some surface structural rearrangement may be responsible for moving these states. Low-energy electron diffraction (LEED)[8,19] studies for the clean surface show only spots that are associated with the ideal (110) surface. This indicates that only structural relaxations which preserve the (110) surface unit cell are possible. Furthermore, the initial interpretation of elastic low-energy electron diffraction (ELEED) data[19] proposed that the (110) surface relaxes into a configuration in which the surface cation attains a planar configuration with its nearest neighbors, holding bond lengths roughly constant.[20] Recent analysis has led to slightly different conclusions about the positions of the surface atoms, although it is still assumed that the surface "buckles" somewhat, displacing the surface anions outward and the surface cations inward. In this section we examine how a variety of surface relaxations, including the configuration initially proposed from ELEED results, affect the intrinsic surface bands. In this way, we may determine whether the observation of no band-gap states is consistent with other types of surface distortions. In addition, we can easily identify structure in the valence band associated with strained bonds on the GaAs (110) surface.

Relaxation alters both the interaction parameters in the surface plane [H_L of Eq. (11)] and the interlayer interaction matrix $\alpha^\dagger$. Calling the new intralayer self-energy at the surface E_{0_s} and the new surface interaction matrix $\alpha_s^\dagger$, we compute the surface density of states $n_s(E)$ from

$$n_s(E) = -\frac{2}{\pi}\int d^2k \,\mathrm{Im}\,\mathrm{Tr}(E - E_{0_s} - \alpha_s^\dagger\, T_2\, \alpha^{-1}\alpha_s)^{-1}\ . \tag{37}$$

The change in bond lengths is taken into account by an exponential enhancement of the interaction parameters of the form

$$V(r') = V(r)e^{-\beta(r'-r)}\ , \tag{38}$$

where β is taken to be 1.89 Å^{-1}. This agrees with an empirical enhancement previously used in tight-binding studies of Si (111) relaxations.[22]

In Fig. 7 we present results for a series of relaxations on the (110) surface. As shown in the right-hand panel, these relaxations (a) shift the surface layer uniformly away from the bulk, (b) shift the surface plane towards the bulk, (c) split the surface anion and cation along the [001] direction, and (d) compress the surface anion and cation along the [001] direction. The relaxations in this figure involve bond-length changes $\lesssim 10\%$.

In Fig. 7(a) we show the surface densities of states for a relaxation which shifts the surface plane uniformly away from the bulk. The associated decrease in interaction parameters causes the anion s band "center of gravity" to shift towards higher energies. Similarly we find the surface resonance near −5 eV to be significantly enhanced. There is also a dramatic enhancement of states near the valence-band maximum.

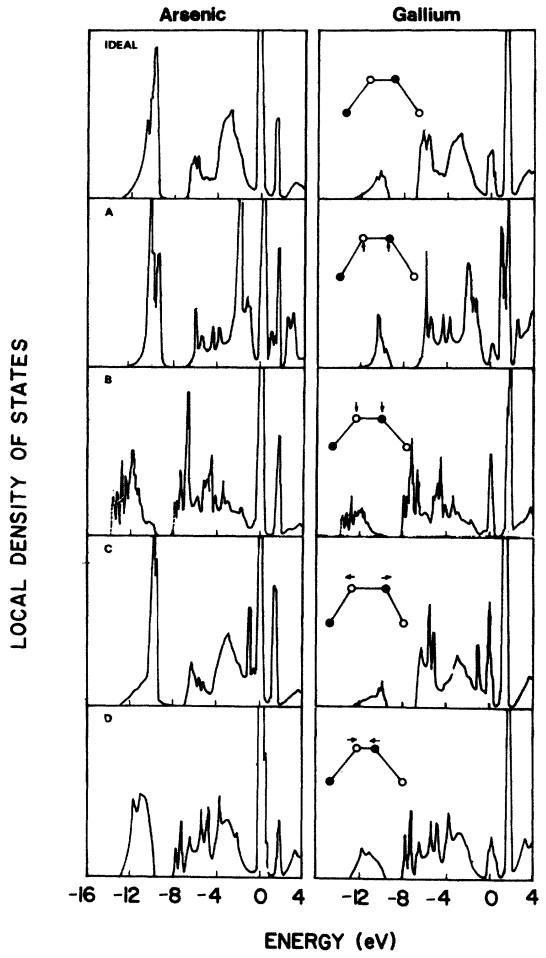

FIG. 7. Densities of states for the ideal (110) GaAs surface and for four structural relaxations given schematically in the left-hand panel. Note that states occur in the band gap for all these configurations.

This is due to weakening of bonds between the surface and "bulk" layers. A striking feature of this spectrum is the broadening of the cation derived surface feature in the upper part of the band gap. The lower edge of this surface band falls about 0.8 eV below the conduction-band edge, and the surface bands on the gap are separated by only ~0.3 eV.

In Fig. 7(b) we show the surface local densities of states in a relaxation which shifts the surface plane uniformly towards the bulk. This relaxation involves a decrease in bond lengths between the surface and bulk layers. The resulting *increase* in the interaction parameters shifts states towards higher-binding energy in the lower s band. In fact, below the bulk-s-band edge, we obtain the tail of an intrinsic surface-state band with a steplike singularity near −14 eV. Similarly, surface-derived features extend into the upper edge of the heteropolar gap near −7.5 eV, exhibiting the steplike singularity. The states found near −3 eV in the ideal configuration are broadened and pushed towards lower energy in this relaxed configuration. We note, however, very slight changes in the band-gap surface states. The relative Ga (As) character is essentially preserved in the relaxation.

In Fig. 7(c) we present results for a relaxation which separates the surface anion and cation along the [001] direction. For such a relaxation, both bond-length and bond-angle variations in the (110) plane affect the surface spectrum. In this configuration we find a shift of states to higher energy in the lowest anionlike s band. We notice a slight enhancement of the resonance near −5 eV in this configuration. An interesting feature of this spectrum is the broadening of the lower band-gap surface state. The character of this state is also changed with this relaxation; roughly 30% of the weight of this state is cationlike. Finally, we also observe a second anionlike peak just below the valence-band maximum. This surface feature is attributed to weakened bonds in the (110) plane.

Finally, in Fig. 7(d) we study a relaxation in which the surface anions and cations are compressed along the [001] direction, "squashing" the zigzag chains in the (110) plane. The resultant strengthening of surface bonds pushes the states in the lowest s-like band to lower energy. We again find states in the upper half of the heteropolar gap, and notice a marked enhancement of the surface states near −5 eV. There is a depletion of states in the p-like region just above −4 eV. In the band gap we find a slight shift of both surface states to higher energy. The lower surface state appears to be more anionlike than the corresponding state in the ideal structure.

This relaxation survey identifies two noteworthy trends. First, we see that the separation and characterization of the dangling-bond surface states is significantly affected by the local interactions. The broadening of the cation-derived band-gap state in Fig. 7(a), and the redistribution of anion and cation character of the band-gap state in Fig. 7(c) demonstrate this point. Secondly, we point to specific features in the valence band which are characteristic of strained surface bonds. In Fig. 7(a) we see that strained back bonds directed towards the bulk result in an enhancement of the valence-band density of states near −2 eV. Similarly, we find an enhancement of states slightly higher in energy near −1 eV to be characteristic of strained bonds in the surface plane. In both cases, weakened surface bonds are evidenced by a shift of states in the lowest valence band toward the heteropolar gap, as previously discussed. As

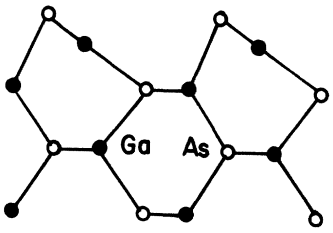

FIG. 8. Surface relaxation which preserves bond lengths, allowing the surface cation to attain a planar configuration with its nearest neighbors.

one would expect, configurations which strengthen these bonds lead to exactly the opposite effects in the energy distributions of surface valence electrons, depleting states from the valence-band edge, pushing states towards higher binding energy in both the first and second valence bands. Finally, we note that the relaxations of the type considered in Fig. 7 are taken to be reasonably large, and yet still fail to move states out of the gap or significantly towards the band edges. We find such distortions to be inconsistent with the observation of no band-gap states on this surface. More importantly, all of these configurations involve bond compression and expansion and hence would not be favored over the sort of relaxation proposed in Ref. 19, which holds bond lengths constant.

This latter relaxation is shown in Fig. 8. In a previous communication, we briefly presented our results for this relaxation of the GaAs surface. Here we will present these results in more detail. From valence arguments, such a relaxation is quite appealing, since we require the threefold coordinated surface anion and cation to bond in natural configurations. That is, the surface As is forming directional bonds at roughly right angles while the Ga forms sp_2 hybridlike interactions with its three coplanar nearest neighbors. From these observations alone and the results of Sec. V we may interpret the effects of such a relaxation. There we noted that the lower band gap state is strongly As p-like in character, directed along the dangling bond. In the relaxed configuration such a dangling orbital is saturated and merges with the bonded p region of the spectrum. The upper gap state shares mixed s and p character on the cation. This relaxation should cause a dehybridization into bonded sp_2-like states and a dangling p-like state. The empty surface state should become more p-like and shift to higher energies.

These trends are verified in the results presented in Figs. 9 and 10. In Figs. 9(a) and 9(b) we show the total density of states for the surface atoms in the unrelaxed and relaxed configurations,

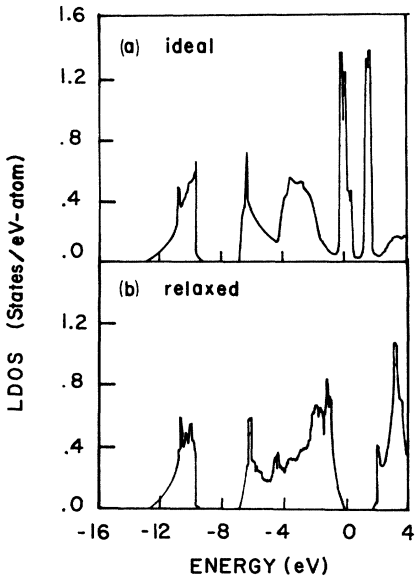

FIG. 9. Surface density of states in (a) the unrelaxed configuration, and (b) the relaxed configuration.

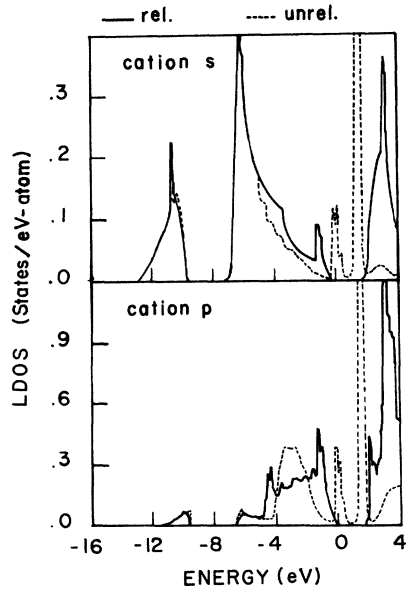

FIG. 10. Projections of surface densities of states onto (a) the surface cation s, and (b) surface cation p orbitals in the unrelaxed configuration and relaxed structure.

respectively. In the relaxed configuration, we note that the surface features have moved out of the gap. The lower As-derived surface band has merged into the valence band forming a broad resonance. Similarly, the cation derived feature has merged into the conduction band with an enhancement of the density of states above the conduction-band edge.

It is interesting to further examine the dehybridization of the upper surface state in this configuration. In Fig. 10, we project the surface densities of states onto cation s and cation p states for both the relaxed and unrelaxed configurations. For the s-state projections, we find an *increase* in the s character of the valence band in the relaxed structure. However, for the p-state partial spectrum, we find that the cation p character of the valence band is essentially unchanged with relaxation. These effects are consistent with the dehybridization model discussed previously. Note, however, that there is still significant s character in the conduction-band surface feature, indicating incomplete dehybridization in this structure.

The two other surface features discussed in Sec. V are found to change slightly with relaxation. The lower of these which is concentrated on the surface anion, with s-like character, shifts to slightly lower energy. In fact, the low-energy anionlike surface band resembles the bulk s band more closely in the relaxed structure. The surface resonance near -6 eV moves slightly higher in energy in the new structure, and the region near -4.5 eV is significantly enhanced with relaxation. This effect is attributable to the increase in cation s character in the valence band in this geometry.

In comparing these results with self-consistent pseudopotential calculations for the relaxed surface[21] we observe the same trends; i.e., the lower band-gap state merges with the valence band and the upper state shifts to higher energy. However, in the pseudopotential calculation, a tail of cation-derived states remains in the upper gap. Within the resolution of our calculation, we find no empty cation-derived gap states in the relaxed geometry.

However, we have noted that the occurrence of such cation-derived features in the gap depends on the parametrization scheme employed.[9] It is noteworthy, however, that a carefully chosen tight-binding Hamiltonian yields results which show trends quite similar to the pseudopotential calculation for the relaxed surface.

Furthermore, the survey shows that the apparent absence of band-gap surface states is consistent only with the sort of drastic relaxation shown in Fig. 8. We find that the dangling-bond surface states move neither out of the gap nor towards the band edges for other types of surface structural rearrangements.

Finally, it is important to point out that in bulk GaAs our tight-binding Hamiltonian predicts a *net* charge transfer of about $0.2e^-$ from the As to the Ga. This means that there are $4.8e^-$ on the As and $3.2e^-$ on the Ga, which strengthens the covalent bonding. This also seems to be substantiated by pseudopotential calculations.[7] On the surface, however, the charge transfer is from the Ga to the As. This implies a repulsion of the surface layer from the next layers into the bulk. We might expect, therefore, that relaxations at the surface should also include a slight outward movement of the surface layer as in relaxation (a) of this section.

VII. CONCLUSIONS

We have shown that using a Hamiltonian of finite range, any semiconducting crystal surface is isomorphic to a terminated linear chain and this may be solved exactly using a method prescribed in Sec. II. We have applied the formalism to the (110) surface of GaAs using a nearest-neighbor tight-binding Hamiltonian. The energy and character of intrinsic surface states calculated in this way agree well with the self-consistent pseudopotential results of Ref. 13. The calculation of a difference spectrum identifies the bulk origins of the surface states, and we have also calculated decay constants for the surface bands.

Using this method we have studied the effects of structural rearrangements on the position and character of surface states. This survey shows that both the position and character of the dangling-bond surface states are significantly affected by the surface configuration. However, we have seen that the observation of few or no band-gap surface states is *only* consistent with a relaxation of the type observed in elastic low-energy electron diffraction experiments. For the Hamiltonian we have studied, such a relaxation yield no empty band-gap surface states. Furthermore, angular projections of the density of states show an incomplete dehybridization of the cation dangling-bond state in the relaxed configuration.

Finally, we emphasize that once the bulk-transfer matrices have been obtained, a wide variety of surface perturbations may be studied easily *without* requiring the rediagonalization of large matrices (as would a finite-slab calculation). In addition to surface structural relaxations, adsorbed molecules, in a variety of bonding configurations, can be treated in this way.

We have extended these realistic tight-binding calculations to oxidation studies at GaAs (110), and are preparing this work for publication.

ACKNOWLEDGMENTS

We thank R. Laughlin for discussions relating to the material in Sec. IV, and Dr. D. J. Chadi for providing us with his unpublished empirical tight-binding parameters. This work was supported in part by the Joint Services Electronics Program, Contract No. DAAB07-76-C-1400. One of us (J.D.J.) was supported in part by the Alfred P. Sloan Foundation.

[1]D. J. Chadi and M. L. Cohen, Phys. Rev. B 11, 732 (1975); K. C. Pandey and J. C. Phillips, *ibid.* 13, 750 (1976).
[2]S. G. Louie and M. L. Cohen, Phys. Rev. B 13, 2461 (1976).
[3]J. A. Appelbaum and D. R. Hamann, Phys. Rev. Lett. 32, 225 (1974).
[4]D. Kalkstein and P. Soven, Surf. Sci. 26, 85 (1971).
[5]L. M. Falicov and F. Yndurain, J. Phys. C 8, 147 (1975).
[6]E. Foo, M. F. Thorpe, D. Weaire, Surf. Sci. 57, 323 (1976).
[7]D. J. Chadi, Phys. Rev. B (to be published).
[8]J. R. Chelikowsky and M. L. Cohen, Phys. Rev. B 14, 556 (1976).
[9]E. J. Mele and J. D. Joannopoulos, Surf. Sci. 66, 38 (1977).
[10]K. C. Pandey, J. L. Freeouf, and D. E. Eastman, J. Vac. Sci. Technol. 14, 904 (1977).
[11]J. D. Joannopoulos and M. L. Cohen, Phys. Rev. B 10, 5075 (1974).
[12](a) C. Calandra and G. Santoro, J. Phys. C 8, L86 (1975); (b) 10, 1911 (1977).
[13]J. R. Chelikowsky and M. L. Cohen, Phys. Rev. B 13, 826 (1976).
[14]J. Van Laar and J. J. Scheer, Surf. Sci. 8, 342 (1967); A. Huijser and J. Van Laar, *ibid.* 52 202 (1975).
[15]D. E. Eastman and J. L. Freeouf, Phys. Rev. Lett. 34, 1624 (1975); P. E. Gregory and W. E. Spicer, Phys. Rev. B 12, 2370 (1975).
[16]W. Gudat and D. E. Eastman, J. Vac. Sci. Technol. 13, 831 (1976).
[17]G. M. Guichar, C. A. Sebenne, and G. A. Garry, Phys. Rev. Lett. 37, 1158 (1976).
[18]L. P. Feinstein and D. P. Shoemaker, Surf. Sci. 3, 294 (1965).
[19]A. R. Lubinsky, C. B. Duke, B. W. Lee, and P. Mark, Phys. Rev. Lett. 36, 1058 (1976).
[20]J. D. Levine and S. Freeman, Phys. Rev. B 2, 3255 (1970); J. E. Rowe, S. B. Christman, and G. Margaritondo, Phys. Rev. Lett. 35, 1471 (1975).
[21]J. R. Chelikowsky, S. G. Louie, and M. L. Cohen, Phys. Rev. B 14, 4724 (1976).
[22]K. C. Pandey and J. C. Phillips, Phys. Rev. Lett. 32, 1433 (1972).